Application of the composite roughness model to high-frequency bottom backscattering

Darrell R. Jackson, Dale P. Winebrenner, and Akira Ishimaru

Citation: The Journal of the Acoustical Society of America **79**, 1410 (1986); doi: 10.1121/1.393669
View online: https://doi.org/10.1121/1.393669
View Table of Contents: http://asa.scitation.org/toc/jas/79/5
Published by the Acoustical Society of America

Application of the composite roughness model to high-frequency bottom backscattering

Darrell R. Jackson
Applied Physics Laboratory, College of Ocean and Fishery Sciences, University of Washington, Seattle, Washington 98105

Dale P. Winebrenner[a)]
Department of Electrical Engineering and Applied Physics Laboratory, University of Washington, Seattle, Washington 98105

Akira Ishimaru
Department of Electrical Engineering, University of Washington, Seattle, Washington 98195

(Received 19 June 1985; accepted for publication 21 January 1986)

The composite roughness model is applied to bottom backscattering in the frequency range 10–100 kHz. For angles near normal incidence, the composite roughness model is replaced by the Kirchhoff approximation which gives better results. In addition, sediment volume scattering is treated, with account taken of refraction and reflection at the randomly sloping interface. In applying the model to published data it is found that sediment volume scattering is dominant in soft sediments except at small and large grazing angles. For coarse sand bottoms, roughness scattering dominates over a wide range of grazing angles. Implications for acoustic remote sensing are discussed.

PACS numbers: 43.30.Bp, 43.30.Dr, 43.30.Gv

INTRODUCTION

Backscattering of centimeter-wavelength sound from the ocean bottom is a process of considerable importance in the operation of underwater acoustic systems. In some cases, bottom backscattering is a major source of interfering reverberation; in other cases, it provides a means of remotely measuring properties of the seafloor.

The purpose of this paper is to develop a model for bottom backscattering, applicable for frequencies from 10–100 kHz. Very little modeling work has been done in this frequency range, but some lower-frequency models appear to be relevant. Table I summarizes the most important features of some representative models[1–9] and serves to place our work in context.

We will first discuss models that treat scattering from the rough water–bottom interface, but neglect scattering from the volume of the sediment. Patterson[1] employed a semiempirical roughness scattering model to describe backscatter data taken at 2.5 kHz. This model displays interesting behavior near the critical angle. A more ambitious model is described by Clay and Medwin.[7] This model is based on the Kirchhoff approximation, with refractive effects approximated by the flat-surface reflection coefficient. This type of model has been applied to bottom remote sensing by Clay and Leong,[10] Dunsiger *et al.*,[11] and Stanton.[12] The Kirchhoff approximation requires that the scattering interface be relatively smooth in the sense that its radii of curvature must not be much smaller than the acoustic wavelength.

The small-roughness perturbation approximation, also known as the Rayleigh–Rice approximation,[13,14] is valid for small radii of curvature, provided the interface relief is much smaller than the acoustic wavelength. This approximation was applied to the sea surface by Marsh and his collaborators.[15–17] The earlier contribution of Miles[18] is directly relevant to the present work, because he considers the refractive two-fluid boundary. The two-fluid perturbation approximation was later applied to bistatic bottom scattering by Kuo,[4] and to bottom forward reflection by Kuperman.[6]

Interface roughness is not the only possible contributor to bottom scattering. A complete model should also consider scattering from within the volume of the sediment, as indicated in Fig. 1. Nolle *et al.*[2] discuss scattering of sound from sediment grains in their experiment conducted at 400–1100 kHz. A simple phenomenological model for the sediment volume scattering process was employed by Zhitkovskii,[5] who took the interface to be nonrefracting and perfectly flat. Refraction and consequent critical angle effects are included in a flat-interface sediment volume-scattering model developed at the Naval Research Establishment (Canada).[3] Crowther[9] has combined Kuo's model for roughness scattering with a volume-scattering model for a flat, refracting interface. He compares this combined model to bottom scattering data below 10 kHz and to the very-high-frequency data of Nolle *et al.*[2] and concludes that sediment volume scattering must be important in soft sediments. Ivakin and Lysanov[8] include refraction at a randomly rough interface in their sediment scattering model. Refraction by large-scale roughness is treated, but diffraction by the smaller scales is neglected.

Modeling of high-frequency ocean surface scattering has received more attention than high-frequency bottom scattering and has exploited results obtained from electro-

[a)] Present address: Max-Planck-Institut für Meterologie, 2000 Hamburg 13, FRG.

 0001-4966/86/051410-13$00.80

TABLE I. Representative bottom scattering models.

Model	Roughness scattering		Volume scattering		
	Boundary condition	Method	Refraction	Interface	Direction
Patterson, 1963[a]	Heuristic	Heuristic	...	...	Back
Nolle *et al.*, 1963[b]	...	...	Two fluid	Flat	Bistatic
Anon., 1963[c]	...	...	Two fluid	Flat	Back
Kuo, 1964[d]	Two fluid	Perturbation	...	...	Bistatic
Zhitkovskii, 1968[e]	...	...	None	Flat	Back
Kuperman, 1975[f]	Two fluid	Perturbation	...	...	Forward
Clay and Medwin, 1977[g]	Approx.	Kirchhoff	...	...	Bistatic
Ivakin and Lysanov, 1981[h]	...	...	Two fluid	Rough	Bistatic
Crowther, 1983[i]	Two fluid	Perturbation	Two fluid	Flat	Back
This model	Two fluid	Composite	Two fluid	Rough	Back

[a] Reference 1. [d] Reference 4. [g] Reference 7.
[b] Reference 2. [e] Reference 5. [h] Reference 8.
[c] Reference 3. [f] Reference 6. [i] Reference 9.

magnetic scattering theory. One of the most successful and widely used models for ocean surface scattering is the composite roughness model, which avoids many of the shortcomings of the Kirchhoff and Rayleigh–Rice approximations by carefully combining the two and treating the interface as the sum of large- and small-scale "surfaces." The large-scale surface must have radii of curvature comparable to or larger than the acoustic wavelength, and the small-scale surface must have relief small compared to the wavelength. For an account of the present state of the composite roughness model as applied to ocean surface acoustic backscattering, the reader should consult the two papers by McDaniel and Gorman.[19,20] McDaniel and Gorman[19] have shown that data on high-frequency surface scattering exhibit clear evidence of volume scattering from a subsurface bubble layer. There is an obvious, but imperfect, analogy between this situation and that encountered in bottom scattering. The analogy is imperfect because, as Fig. 1 illustrates, sound energy impinging on the bottom encounters a rough, refracting interface before and after it is scattered by volume inhomogeneities in the sediment.

In rough-surface scattering, it is common to deal with the scattering cross section per unit area. This is defined with reference to a finite patch of the surface large enough to embody the essential statistical properties of the entire surface. The expected value of the scattered intensity I_s is computed for a range r from the patch sufficient to insure spherical spreading. If I_0 is the incident intensity, the scattering cross section per unit solid angle per unit area of scattering surface is

$$\sigma = r^2 I_s / I_0 A, \tag{1}$$

where A is the area of the patch. For the sake of brevity, we will refer to σ as the scattering cross section, even though it does not have the dimensions of area. Clay and Medwin[7] use the term "scattering function" for this quantity. The above definition is general enough to include bistatic scattering, but we have need for only the monostatic case. It is noteworthy that σ is dimensionless and therefore is independent of the unit system employed. The quantity $10 \log \sigma$ is called the *scattering strength*[21] and is expressed in decibels without reference to a unit of length.

In modeling bottom scattering, we will compute σ separately for interface roughness and sediment volume scattering and then add the two cross sections. The approximations that are inherent in this approach will be discussed in the section on volume scattering.

In Sec. I, we give a brief description of those bottom properties, such as sound speed in the sediment and roughness spectra, that appear to be relevant to the bottom scattering problem. Section II introduces the perturbation approximation for the rough two-fluid interface and Sec. III describes the corresponding composite roughness model, with particular attention to criteria for its validity. Section IV is devoted to application of the Kirchhoff approximation for steep grazing angles, where it is superior to the composite roughness approximation. Section V discusses a sediment volume scattering model that is similar to that of Ivakin and Lysanov[8] in its treatment of the rough interface. A comparison between models and experimental data is given in Sec. VI. Finally, Sec. VII draws conclusions about the usefulness and shortcomings of the various models and about the relative importance of interface roughness and sediment volume scattering at high frequencies.

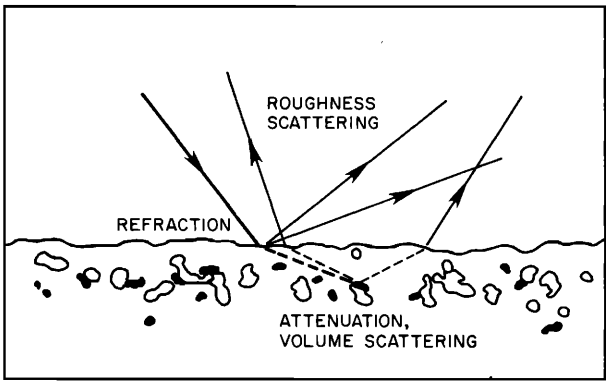

FIG. 1. Bottom acoustic scattering mechanisms, including refraction and scattering at the water–bottom interface and attenuation and scattering in the sediment.

I. BOTTOM PROPERTIES

In the models to be developed, the sediment is idealized as an acoustically refractive and lossy fluid, homogeneous except for small-scale variations in sound speed and mass density responsible for volume scattering. Although this picture is certainly oversimplified, it is a reasonable starting point, because sound attenuation at high frequencies limits penetration to a few meters or less in most cases. The attenuation coefficient increases with frequency and values on the order of 1–100 dB m^{-1} are typical in the 10–100 kHz frequency range.[22] This makes it possible in most cases to ignore underlying rock, which can support shear waves. Gradients or layering on scales of a meter or less may be important in some cases, but will be ignored. For such an idealized sediment, the volume parameters of interest are compressional wave attenuation and speed, mass density, and volume scattering strength. Even though attenuation is large enough to prevent deep penetration into the sediment, sediment attenuation loss is small in the sense that the imaginary part of the wavenumber is much smaller than the real part. Available data[22] yield ratios of imaginary to real wavenumbers between 0.3 and 0.015. This fact will permit the neglect of attenuation in certain parts of the modeling problem.

A good summary of data on compressional wave speed and mass density has been given by Hamilton and Bachman.[23] In the shallow waters of the continental shelf, the ratio of compressional wave speeds in the sediment to the overlying water is usually somewhat greater than unity, which causes refraction away from the normal. For grazing angles shallower than the "critical angle" at which the refracted ray becomes horizontal, penetration into a flat bottom will be negligible, and volume scattering should be unimportant. Very fine sediments, such as clay, may have speed ratios slightly less than unity, and may exhibit an angle of intromission (see, e.g., Ref. 21, p. 128) rather than a critical angle when the bottom is flat.

The mass density of continental shelf sediments is typically in the range one to two times that of seawater. Mass density and compressional wave speed ratios are highly correlated, with soft, fine silts and sands having values for both ratios close to unity and coarser sands having larger values. Biological or hydrodynamic activity can loosen the uppermost sediment, causing marked reduction in these ratios.[24,25] Such effects are of particular importance at high frequencies, where acoustic interaction takes place very near the interface.

We are unaware of any published data on sediment volume scattering measurements at high frequencies. For centimeter-length acoustic waves, it is likely that the most important inhomogeneity is not the graininess of the sediment, but larger-scale inhomogeneities such as those caused by burrowing and shells. Crowther[9] finds that available data on sediment inhomogeneity have insufficient spatial resolution to allow calculation of volume scattering strengths for frequencies above 4 kHz. We will treat sediment volume scattering strength as a free parameter to be determined by fits to bottom backscatter data. No attempt will be made to identify the type of inhomogeneity responsible for scattering.

Most data on bottom roughness are derived from bathymetry having a resolution of 100 m or larger.[26–28] Two-dimensional roughness spectra with centimeter-scale resolution have been measured by Akal and Hovem.[29] One-dimensional spectra with centimeter-scale resolution presented by Igarashi and Allman,[30] Jackson *et al.*,[31] and Fox and Hayes[28] agree with the lower resolution data in having power-law roughness spectra. One important issue yet to be resolved is whether typical bottoms can be described by a single power-law spectrum that spans both very small and very large scales. Fox and Hayes[28] have shown that this is approximately true for one area, but more data are needed before general conclusions can be drawn. Random processes with true power-law spectra require careful treatment, as they are nonstationary and may not possess some of the common statistical measures such as moments and correlation lengths. Such processes are special cases of *stationary increment* processes (Ref. 32 and Appendix B of Ref. 33). In the present context, the random process of interest is the bottom profile $h(\mathbf{r})$, where $\mathbf{r}$ is the two-dimensional vector giving horizontal position. The term *stationary increment* implies that, while $h(\mathbf{r})$ may not be stationary, the random process defined as the difference $h(\mathbf{r}+\mathbf{r}_0)-h(\mathbf{r}_0)$ is stationary, where $\mathbf{r}_0$ is an arbitrary horizontal displacement. In practical terms, this approach is useful when the relief has both small- and large-scale components, but the largest scales are well beyond the range of interest. For example, the largest scales may be geographic in size and of no interest in the high-frequency scattering problem. This situation is complementary to that envisioned by Clay and Leong[10] and Stanton,[12] who assume that the correlation length and rms surface height are small enough to be measured by means of lower-frequency acoustics. The choice of one approach or the other should be based at least in part on a comparison of the known or estimated roughness scales with the acoustic wavelength.

Because the relief spectra for the experimental sites of interest exhibit power-law behavior, we find it convenient to use the stationary increment formalism, except in instances where filtered, stationary versions of the interface relief are considered, as in the small-scale portion of the composite-roughness model.

We will assume that the two-dimensional roughness statistics are Gaussian and isotropic with spectrum of the form

$$W(\mathbf{k}) = \beta k^{-\gamma}. \tag{2}$$

In this expression, $\mathbf{k}$ is a two-dimensional wave vector with magnitude equal to the wavenumber k. The high-resolution bottom data of interest[30,31] have $\gamma = 3$–3.5. The restriction to power-law spectra with isotropic statistics is made for simplicity and excludes, e.g., bottoms with directional sand ripples. The more general anisotropic case can be treated without excessive difficulty. It would not be easy to proceed without the assumption of Gaussian statistics. Published work on centimeter-scale bathymetry is unavailable to support this assumption, but it appears to be valid at least for one set of data.[34] Problems arising from non-Gaussian statistics will be discussed later in this paper.

The spectrum $W(\mathbf{k})$ is related to the structure function

$D(\mathbf{r})$. The structure function is defined as the expected value of the square of the increment in $h(\mathbf{r})$ for fixed horizontal displacement:

$$D(\mathbf{r}) = E\{[h(\mathbf{r}+\mathbf{r}_0) - h(\mathbf{r}_0)]^2\}. \quad (3)$$

The spectrum and structure function are connected by the following transformation:

$$D(\mathbf{r}) = 2\int_{-\infty}^{\infty}\int_{-\infty}^{\infty}(1-\cos\mathbf{k}\cdot\mathbf{r})\,W(\mathbf{k})\,d^2k. \quad (4)$$

We do not need the inverse relationship giving the spectrum in terms of the structure function, but the interested reader may consult Ishimaru (Appendix B).[33]

If the roughness statistics are isotropic, the spectrum and the structure function will depend only on the magnitudes k and r of the two-dimensional vectors $\mathbf{k}$ and $\mathbf{r}$. The structure function corresponding to the isotropic spectrum of Eq. (2) is

$$D(\mathbf{r}) = C_h^2 r^{2\alpha}, \quad (5)$$

where

$$C_h^2 = [2\pi\beta\Gamma(2-\alpha)2^{-2\alpha}]/[\alpha(1-\alpha)\Gamma(1+\alpha)] \quad (6)$$

and

$$\alpha = (\gamma/2) - 1. \quad (7)$$

The integral in Eq. (4) is convergent for $0<\alpha<1$.

The structure function provides a measure of roughness that is easier to interpret, in some respects, than the power spectrum. For the bottom, reasonable values for the structure function parameters are $\alpha\approx 0.63$, $C_h r^{\alpha}\approx 3$ cm at $r = 100$ cm. In other words, the rms height difference for points separated by 100 cm is about 3 cm. If we assume the power law holds at larger scales, it follows that the rms height difference increases rather slowly as separation increases, being only about 60 cm at 100 m separation and about 2.5 m at 1000 m separation. Topographic changes of this magnitude are quite reasonable.

Stationary processes are special cases of stationary increment processes, so Eqs. (3) and (4) are also useful in cases where such statistical measures as rms relief, covariance, and correlation length have meaning. If the two-dimensional relief $h(\mathbf{r})$ is a stationary process having zero expected value

$$E\{h(\mathbf{r})\} = 0, \quad (8)$$

then the covariance is

$$B(\mathbf{r}) = E\{h(\mathbf{r}+\mathbf{r}_0)h(\mathbf{r}_0)\}. \quad (9)$$

In this case,

$$D(\mathbf{r}) = 2[\beta(0) - B(\mathbf{r})], \quad (10)$$

$$W(\mathbf{k}) = \frac{1}{(2\pi)^2}\int_{-\infty}^{\infty}\int_{-\infty}^{\infty}\exp(i\mathbf{k}\cdot\mathbf{r})B(\mathbf{r})\,d^2r. \quad (11)$$

We will later have need for the following spectrum normalization result:

$$\int_{-\infty}^{\infty}\int_{-\infty}^{\infty}W(\mathbf{k})\,d^2k = h^2, \quad (12)$$

where

$$h^2 = B(0) \quad (13)$$

is the mean-square relief, defined only when the interface relief is a stationary random process with a non-power-law spectrum.

II. RAYLEIGH–RICE APPROXIMATION

The composite roughness model applies the Rayleigh–Rice perturbation approximation to the small-scale portion of the interface. This approximation is valid if the small-scale rms relief is much smaller than the acoustic wavelength. The fact that one must consider the rms relief implies that the small-scale surface cannot have a power-law spectrum extending to arbitrarily low wavenumbers. This is insured in the composite roughness model by the filtering operation used to define the small-scale surface.

Most treatments of rough-surface perturbation theory assume an impenetrable boundary that is either a pressure release or hard surface.[15–17,35,36] For the penetrable, two-fluid interface, one must impose continuity of pressure and the normal component of velocity across the interface and then solve for the scattered field to first or second order in the relief $h(\mathbf{r})$.[4,6] A first-order calculation is sufficient to obtain the expected value of the scattered intensity, from which the scattering cross section can be obtained. We will employ Kuo's[4] backscattering cross section, the acoustic analog of results derived for the electromagnetic case by Barrick and Peake.[37]

The sediment is taken to be a homogeneous fluid characterized by its mass density and compressional wave speed. Losses are neglected on the grounds that the imaginary part of the wavenumber is usually much smaller than the real part at the frequencies of interest. It is convenient to introduce the following ratios defining the essential sediment properties:

$$\nu = \frac{\text{sediment compressional wave speed}}{\text{water sound speed}}, \quad (14)$$

$$\rho = \frac{\text{sediment mass density}}{\text{water mass density}}. \quad (15)$$

The small-scale backscattering cross section $\sigma_s(\theta)$ depends upon these quantities as well as upon the grazing angle θ and the acoustic wavenumber in water $k_a = \omega/c$. Assuming without loss of generality that the incident wave vector is parallel to the x–z plane, and introducing the notation $W(k_x, k_y) = W(\mathbf{k})$, Kuo's cross section expression can be expressed in our notation as

$$\sigma_s(\theta) = 4k_a^4\sin^4\theta F(\theta,\nu,\rho)W(2k_a\cos\theta,0). \quad (16)$$

This expression singles out a specific wavenumber in the two-dimensional roughness spectrum, the Bragg wavenumber $2k_a\cos\theta$. Use of the term "Bragg wavenumber" does not imply that the rough surface must be periodic; it simply means that, out of the entire spectrum of interface wavelets, those having the Bragg wavenumber dominate backscattering when surface relief is much smaller than the acoustic wavelength. As long as the interface relief is small, Eq. (16) has a wide range of validity, including anisotropic and non-Gaussian interfaces, but we only consider the isotropic Gaussian case.

The form of the function $F(\theta,\nu,\rho)$ changes as the grazing angle passes the critical angle θ_c:

$$\theta_c = \cos^{-1}(\nu^{-1}), \tag{17}$$

$$F(\theta,\nu,\rho) = \begin{cases} \dfrac{[(\rho-1)^2\cos^2\theta + \rho^2 - \nu^{-2}]^2}{[\rho\sin\theta + (\nu^{-2}-\cos^2\theta)^{1/2}]^4}, & \theta > \theta_c \\ \dfrac{[(\rho-1)^2\cos^2\theta + \rho^2 - \nu^{-2}]^2}{[(1-\rho^2)\cos^2\theta + \rho^2 - \nu^{-2}]^2}, & \theta < \theta_c. \end{cases} \tag{18}$$

If $\nu < 1$, the sound speed in the sediment is slower than the sound speed in the overlying water and there is no critical angle. In this case, the $\theta > \theta_c$ version of $F(\theta,\nu,\rho)$ should be used. Figure 2 displays curves of scattering strength ($10\log\sigma_s$) computed from Eq. (16) using sound speed and density ratio values that are typical for sediments ranging from silty clay to coarse sand. Also shown in Fig. 2 are curves for the pressure-release boundary ($\rho\to 0$) and the hard boundary ($\rho\to\infty$). The roughness spectrum employed in Fig. 2 is given by Eq. (2) with $\beta = 4\times 10^{-3}$ and $\gamma = 4$. This is a convenient choice for γ because it makes scattering strength independent of frequency. In actuality, one should consider that γ is slightly less than 4, to avoid problems with convergence of the integral in Eq. (4). A strong cusp is seen at the critical angle, with scattering strength decreasing sharply as the grazing angle increases past the critical value. This decrease indicates that the boundary becomes relatively transparent for angles where penetration is possible. The cusp occurring at the critical angle is blurred in the composite roughness model because of the dependence of the local grazing angle on the random large-scale slope. Exponent values $\gamma = 3$–3.5 are more appropriate for high-frequency bottom scattering than $\gamma \approx 4$. The smaller exponents cause scattering strength to increase with frequency at rates of 1.5–3 dB per octave and give curves with virtually the same shape as Fig. 2.

III. COMPOSITE ROUGHNESS MODEL FOR MODERATE GRAZING ANGLES

Brown[38,39] and McDaniel and Gorman[20] give derivations and references for the composite roughness model for impenetrable surfaces. Our approach for the penetrable, two-fluid boundary will be heuristic, borrowing results from the simpler pressure release case without rigorous justification. The composite roughness expression for the scattering cross section contains two terms, one of which we will ignore for the present, as it is only important at large grazing angles. Figure 3 illustrates the essential idea of the composite roughness model as applied to moderate grazing angles. The model assumes that backscattering is due to small-scale roughness, with local grazing angle dependent on the slope of the large-scale surface. The local grazing angle θ_g is related to the true grazing angle θ and to the two components h_x and h_y of large-scale slope as follows:

$$\sin\theta_g = (\sin\theta + h_x\cos\theta)/(1 + h_x^2 + h_y^2)^{1/2}. \tag{19}$$

It is assumed that the rms slope s of the large-scale surface is small,

$$s < 0.1. \tag{20}$$

A restriction will be made to grazing angles less than 70° so that the local grazing angle can be approximated as $\theta + h_x$, as indicated in Fig. 3.

Assuming that the slope of the large-scale surface is a Gaussian-distributed random variable, the backscattering cross section for grazing angles of order 70° and less is obtained by averaging the small-scale backscattering cross section as follows:

$$\sigma(\theta) = \frac{R(\theta,s)}{\pi^{1/2}s}\int_{-\theta}^{\infty}\sigma_s(\theta + h_x)\exp\left(-\frac{h_x^2}{s^2}\right)dh_x. \tag{21}$$

The function $R(\theta,s)$ accounts for shadowing by the large-scale surface. Following McDaniel and Gorman,[19] we will use the shadowing function derived by Wagner[40]:

$$R(\theta,s) = (2Q)^{-1}(1 - e^{-2Q}), \tag{22}$$

where

$$t = s^{-1}\tan\theta, \tag{23}$$

$$Q = (1/4t)[\pi^{1/2}e^{-t^2} - t(1 - \operatorname{erf} t)], \tag{24}$$

and erf is the error function.

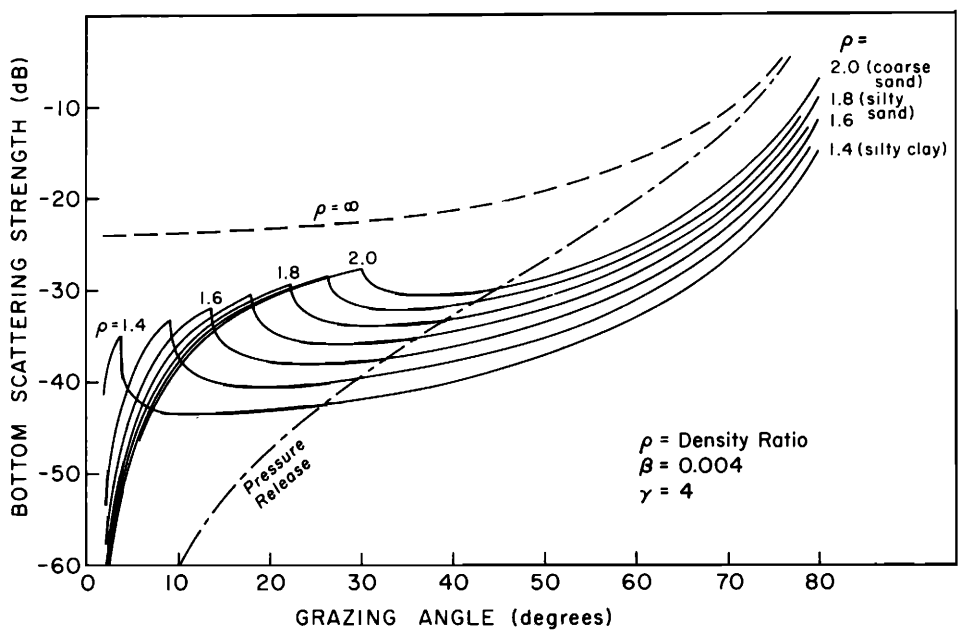

FIG. 2. Small-scale roughness scattering strength computed in the Rayleigh–Rice approximation for a two-fluid interface. The density and sound speed ratios used in these calculations are $(\rho,\nu) = (1.4, 1.002), (1.5, 1.013), (1.6, 1.029), (1.7, 1.052), (1.8, 1.081), (1.9, 1.116)$, and $(2.0, 1.157)$.

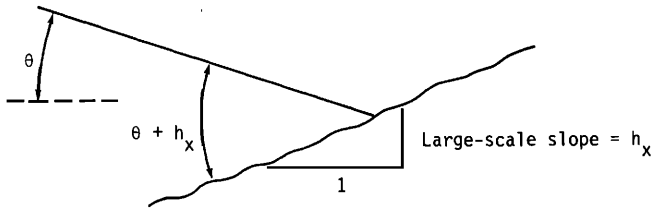

FIG. 3. The large-scale slope averaging process used in the composite roughness model. The local grazing angle is dependent on the local value of the large-scale slope.

The roughness spectrum must be partitioned into large- and small-scale parts, as indicated in Fig. 4. The cutoff wavenumber k_c marks the boundary between the two parts and must be chosen so that the small-scale surface satisfies the conditions for validity of the perturbation, or Rayleigh–Rice approximation. In addition, the cutoff must be chosen so that the large-scale surface can be treated as locally flat, as implicit in the above discussion. The condition on the small-scale surface will be taken to be

$$2k_a h_s < 1. \tag{25a}$$

Conditions similar to this have been presented by Bachmann,[41] Bass and Fuks,[42] Burrows,[43] Labianca and Harper,[35] Brown,[38] and Winebrenner.[44] The quantity h_s is the rms relief of the small-scale surface, and k_a is the acoustic wavenumber. Some authors[4,33,45] give more relaxed conditions for validity of the perturbation approximation. Up to a numerical factor, these are of the form

$$2k_a h_s \sin\theta < 1. \tag{25b}$$

Owing to uncertainty as to the most suitable Rayleigh–Rice criterion, we will present numerical results based on both Eqs. (25a) and (25b), referring to the latter case as the "extended" model.

Given the spectral normalization specified in Eq. (12), the small-scale rms relief appearing in the Rayleigh–Rice criteria can be calculated in terms of the spectrum as follows:

$$h_s^2 = 2\pi \int_{k_c}^{\infty} W(\mathbf{k}) k \, dk. \tag{26}$$

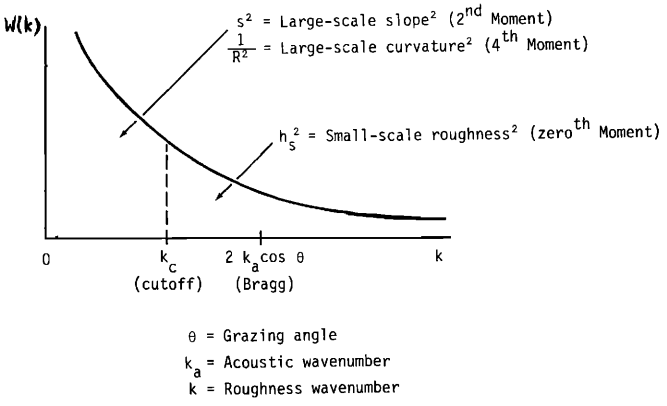

FIG. 4. Composite roughness filtering of the roughness spectrum with cutoff wavenumber separating the large- and small-scale parts of the spectrum.

Implicit in this expression is the definition of the small-scale interface relief as a filtered version of the true interface relief. The filter has unit frequency response outside the circle $k = k_c$ and has zero frequency response inside this circle. This filtering operation removes the low frequencies responsible for nonexistence of the covariance.

The large-scale surface is defined by a filtering operation complementary to that used for the small-scale surface, with zero frequency response outside the circle $k = k_c$. The large-scale surface must satisfy a condition on radius of curvature R. This condition will be taken in the form

$$[2/(k_a R \sin^3\theta)] < 1. \tag{27}$$

This constraint arises in the derivation of the composite roughness model through application of the Kirchhoff approximation to the large-scale surface.[20] Motivation for the form of Eq. (27) can be found in the work of Liszka and McCoy.[46] The conditions on small-scale relief and large-scale curvature are not as well founded and definite as one would like, owing to the extreme difficulty of estimating errors resulting from the various assumptions. McDaniel and Gorman[20] provide some useful estimates of error for ocean surface scattering, but similar calculations have not been carried out for the two-fluid case. Rigorous versions of the above inequalities would depend on the sound speed and density ratios, but, lacking a rigorous error analysis, we will proceed on the basis of Eqs. (25) and (27).

McDaniel and Gorman[20] derive additional criteria for the validity of the composite roughness model as applied to sea-surface scattering. We have considered these criteria in the context of the present problem and find that they do not impose any additional constraints on the choice of the cutoff wavenumber.

In the following, we will define a measure of the mean-square curvature of the large-scale surface for use in the Kirchhoff criterion. It is necessary to consider the following statistical moments:

$$h_s^2 = E\{h_s^2(\mathbf{r})\}, \tag{28}$$

$$s^2 = E\{[\partial_x h_l(\mathbf{r})]^2 + [\partial_y h_l(\mathbf{r})]^2\}, \tag{29}$$

$$R^{-2} = E\{[\partial_x^2 h_l(\mathbf{r})]^2 + 2[\partial_{xy}^2 h_l(\mathbf{r})]^2 + [\partial_y^2 h_l(\mathbf{r})]^2\}. \tag{30}$$

The subscripts s and l stand for the small- and large-scale surfaces, respectively. The rms relief h_s of the small-scale surface is used in the Rayleigh–Rice criteria; the rms slope s of the large-scale surface is needed for the slope averaging process; and the radius of curvature R is used in the Kirchhoff criterion. Equation (30) was obtained by forming the sum of the inverse squares of the two principal radii of curvature, making a small-slope approximation, and taking the ensemble average of the result.

These moments can be expressed in terms of the spectrum by Fourier transforming appropriate derivatives of the covariance and integrating by parts. When applied to Eq. (28), this procedure yields Eq. (26). Equations (29) and (30) give the following:

$$s^2 = 2\pi \int_0^{k_c} W(\mathbf{k}) k^3 \, dk, \tag{31}$$

$$R^{-2} = 2\pi \int_0^{k_c} W(\mathbf{k}) k^5 \, dk. \tag{32}$$

Equations (26), (31), and (32) were simplified by assuming isotropy and are readily evaluated for the power-law spectrum of Eq. (2):

$$h_s^2 = (2\pi\beta k_c^{2-\gamma})/(\gamma - 2), \tag{33}$$

$$s^2 = (2\pi\beta k_c^{4-\gamma})/(4 - \gamma), \tag{34}$$

$$R^{-2} = (2\pi\beta k_c^{6-\gamma})/(6 - \gamma). \tag{35}$$

Figure 5 shows the dependence of these quantities on the cutoff wavenumber with parameters β and γ appropriate to some of the measurement sites of Jackson *et al.*[31] The cutoff must be chosen in such a fashion that rms relief, slope, and curvature simultaneously satisfy the criteria given in Eqs. (20), (25), and (27).

There is some ambiguity in choosing the cutoff, but the range of choice can be narrowed by imposition of additional constraints. For example, Brown[38] and McDaniel and Gorman[19] favor the Rayleigh–Rice criterion [Eq. (25)] in their treatments of sea-surface scattering by placing the cutoff wavenumber at a high value in order to obtain a low value for the small-scale relief. Given measured bottom roughness spectra, we find it difficult to satisfy the Kirchhoff criterion, owing to large curvatures originating in the high-frequency part of the roughness spectrum. As a result, we will favor the Kirchhoff criterion by placing the cutoff so that the Rayleigh–Rice criterion [Eq. (25a)] is barely satisfied. The composite roughness model will then be valid over the grazing angle interval from 70° down to the smallest angle satisfying Eq. (27). In addition, we will consider the less stringent Rayleigh–Rice criterion [Eq. (25b)]. At small grazing angles, this criterion can be satisfied by very small cutoff wavenumbers, which yield large values for the radius of curvature of the large-scale surface. By separately considering several such cutoffs, we can extend the model to small grazing angles. We will later give numerical results for this "extended" model, which we consider provisional, subject to a better understanding of the various criteria discussed above.

As mentioned earlier, the power-law spectrum requires careful interpretation as rms height, slope, and curvature become infinite. These problems do not arise in our application, where filtering eliminates such infinities. Even with filtering, the rms height of the large-scale surface and the rms slope and curvature of the small-scale surface are infinite. These quantities are not needed for the composite roughness model, but they can be estimated if the spectrum is known to fall below the power-law approximation at very low and very high wavenumbers. Additional cutoffs at these extreme wavenumbers can be introduced in the limits of the integrals (26), (31), and (32). The effects will be small as long as the additional cutoffs are a decade or more removed from the composite roughness cutoff k_c.

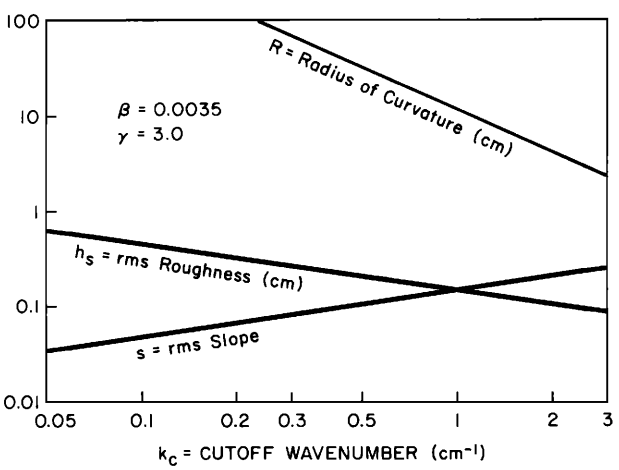

FIG. 5. Composite roughness model parameters as functions of the cutoff wavenumber.

IV. KIRCHHOFF APPROXIMATION FOR STEEP GRAZING ANGLES

The preceding discussion of the composite roughness model was based on the assumption that the grazing angle was about 70° or less. At steeper angles, application of the composite roughness model is more complicated and open to question. The complications are not a major problem. Equation (21) is replaced by an averaging integral that takes into account the dependence of the local grazing angle on *both* components of the large-scale slope, and scattering by the large-scale surface adds a second term to Eq. (21). This second term is obtained by applying the so-called facet model to the large-scale surface. McDaniel[47] has shown that the composite roughness model in this form is faulty when applied to sea-surface scattering at steep grazing angles, because the sum of these two terms is unduly dependent on the cutoff. This dependence arises because the facet model ignores diffraction by the large-scale surface, which becomes significant at steep grazing angles.

We have performed similar calculations which show that the situation is also bad for high-frequency bottom backscattering at steep grazing angles. This problem can be remedied by making diffractive corrections to the facet model.[47] We will follow a different course, replacing the *entire* composite roughness model by the Kirchhoff approximation at steep grazing angles. This is possible because the Kirchhoff criterion [Eq. (27)] is much less stringent at steep grazing angles, making it unnecessary to subtract the short-wavelength portion of the interface before applying the Kirchhoff approximation. Berry and Blackwell[48] have shown that the power-law spectrum in the Kirchhoff approximation produces finite results without resort to cutoffs of any kind. Our approach differs from that of Berry and Blackwell in focusing on the scattering cross section rather than the asymptotic time dependence of intensity.

Considering the definition of scattering strength [Eq. (1)], the scattered intensity is usually taken to be the incoherent intensity, defined as the total intensity minus the coherent intensity. The coherent intensity is defined as the square of the expected value of the scattered field. When the rough-surface relief is comparable to or greater than the acoustic wavelength, the coherent intensity is usually a negligible fraction of the total intensity. This is the situation of interest here.

In the Kirchhoff approximation, the backscattering

cross section when the coherent intensity is negligible is given by the expression

$$\sigma(\theta) = \left(\frac{k_a g(\pi/2)}{2\pi \sin\theta}\right)^2 \int_{-\infty}^{\infty}\int_{-\infty}^{\infty} \exp[2ik_a \cos\theta x - 2k_a^2 \sin^2\theta D(\mathbf{r})]d^2r. \quad (36)$$

Equation (36) is derived using integration by parts (see, e.g., Ref. 33) in order to avoid the small-slope assumption employed by many authors. In Eq. (36) $\mathbf{r} = (x, y)$ and the coordinate x is in the vertical plane containing the incident wave vector. The parameter $g(\pi/2)$ is the plane-wave reflection coefficient for normal incidence

$$g(\pi/2) = (\rho v - 1)/(\rho v + 1). \quad (37)$$

Using the power-law structure function given by Eq. (5) in Eq. (36), transforming to polar coordinates, and performing the angular integral, one obtains the following result:

$$\sigma(\theta) = \frac{g^2(\pi/2)}{8\pi \sin^2\theta \cos^2\theta}\int_0^{\infty} \exp(-qu^{2\alpha})J_0(u)u\,du, \quad (38)$$

where

$$q = \sin^2\theta \cos^{-2\alpha}\theta C_h^2 2^{1-2\alpha} k_a^{2(1-\alpha)}, \quad (39)$$

and where $J_0(u)$ is the zeroth-order Bessel function of the first kind. We have evaluated the integral in Eq. (38) numerically for various choices of the parameters q and α. Figure 6 shows the dependence of the scattering strength on the power-law exponent with a fixed value for the parameter C_h. The scattering strength curve for $\alpha = 0.5$ is sharply peaked at vertical incidence, while the curve for $\alpha = 1.0$ is much broader. The integral in Eq. (38) can be performed analytically for both of these special cases. The limit $\alpha = 0.5$ corresponds to $\gamma = 3.0$, a spectrum rich in high frequencies. A two-dimensional vertical slice through such a surface has the same statistical properties as the time series for the position of a particle undergoing Brownian motion in one dimension. The limit $\alpha = 1.0$ corresponds to $\gamma = 4.0$, a surface "smoother" than the bottoms considered here. Values $\alpha = 0.5$–0.75 give reasonable approximations to the roughness data cited in Sec. I.

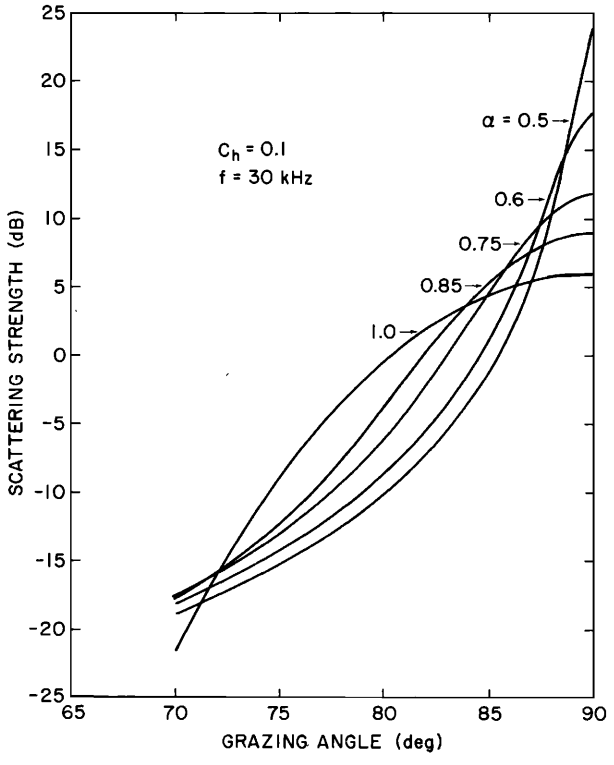

FIG. 6. Backscattering strength near vertical incidence computed in the Kirchhoff approximation for different power-law exponents. The reflection coefficient is assumed to be unity.

Several questions arise regarding the validity of the Kirchhoff approximation with power-law roughness spectrum. Easiest to answer is the mathematical question regarding finiteness of results obtained using a spectrum that has no finite moments. The integral in Eq. (38) is obviously finite over our range of interest $0.5 < \alpha < 1.0$. Furthermore, the main contribution to this integral comes from the region where the real exponent in Eq. (38) is of order unity:

$$2k_a^2 \sin^2\theta D(\mathbf{r}) \approx 1. \quad (40)$$

With typical bottom roughness parameters and centimeter wavelengths, this corresponds to length scales of about 10 cm, where the spectrum and structure function are experimentally well established.

It is necessary to consider the Kirchhoff criterion in the present case. The power-law spectrum gives infinite curvature, but this is owing to infinitely short wavelets that cannot be important because they make no contribution to surface relief. Similarly, the power-law spectrum gives infinite slope, but the existence of the surface-slope terms mentioned earlier makes it clear that the Kirchhoff approximation is only applicable to differentiable surfaces. To understand the nature of the small-scale part of the spectrum responsible for large curvatures and slopes, consider a two-scale filtering operation in which the small-scale portion of the surface will be discarded as an approximation and the large-scale portion will be treated in the Kirchhoff approximation. The cutoff will be placed such that the slope of the remaining large-scale surface is finite and the curvature just satisfies the Kirchhoff criterion [Eq. (27)]. For spectral parameters appropriate to the present application, the rms relief of the small-scale surface thus defined is about one-tenth the acoustic wavelength. Furthermore, the cutoff is several times larger than the Bragg wavenumber associated with backscattering at grazing angles larger than 70°. Since the small-scale surface has very small relief and none at the Bragg wavenumber, its neglect is justified.

Another concern has to do with the farfield, or spherical spreading, assumption that is contained in the definition of scattering strength [Eq. (1)] and is necessary in deriving Eq. (36) from the Kirchhoff approximation. Several authors have considered the conditions under which the farfield assumption is valid, given a finite surface correlation length and an illuminated patch that is larger than the surface correlation length (see, e.g., Refs. 49–52 and references therein). A rough interface with power-law spectrum has infinite correlation length and this causes one to question whether it is possible to define the patch discussed in connection with Eq. (1). A recent paper by Winebrenner and Ishimaru[53] shows that the size of this patch is not constrained by the

surface correlation length, but must be larger than the correlation length of the *surface field*. For a very rough surface, the surface field correlation length can be much smaller than the surface correlation length owing to the randomization of phase caused by relief comparable to or greater than the acoustic wavelength. Thus it appears that the required patch size need not approach infinity as the surface correlation length approaches infinity and that the power-law spectrum does not prevent use of the farfield approximation in defining the scattering strength.

Having established the validity of separate models for interface scattering at moderate and steep grazing angles, we will finally consider a model for sediment volume scattering.

V. SEDIMENT VOLUME SCATTERING

The NRE[3] volume scattering model includes refraction and attenuation in a statistically homogeneous sediment with perfectly flat interface. The resulting surface scattering strength is

$$\sigma_{vs}(\theta) = \begin{cases} \dfrac{5\sigma_v[1-g^2(\theta)]^2\sin^2\theta}{\alpha_b \ln 10 \sin\theta_b}, & \theta > \theta_c, \\ 0, & \theta < \theta_c. \end{cases} \tag{41}$$

The subscript v stands for "volume" while the subscript s stands for "small scale," analogous to Eq. (16). We will return to this analogy after defining the remaining quantities in Eq. (41). The scattering cross section per unit solid angle per unit sediment volume is denoted σ_v, and α_b is the compressional wave attenuation coefficient expressed in decibels per unit length. Acoustic rays refracted at the flat interface make an angle θ_b with respect to the horizontal, where

$$\sin\theta_b = [1-(v\cos\theta)^2]^{1/2}, \tag{42}$$

provided the grazing angle is larger than the critical angle. The plane-wave reflection coefficient appears in Eq. (41) and is

$$g(\theta) = (\rho v \sin\theta - \sin\theta_b)/(\rho v \sin\theta + \sin\theta_b). \tag{43}$$

The surface scattering cross section $\sigma_{vs}(\theta)$ depends on the ratio σ_v/α_b. We will treat this ratio as a free parameter and will not attempt to relate it to specific scattering mechanisms. Equation (41) is valid in the single scattering regime, which is analogous to the first-order perturbation regime for which the small-scale roughness scattering expression (16) is applicable. We will carry this analogy even further by averaging over large-scale slope with shadowing in precisely the same way as was done in the composite roughness model [Eq. (21)]. This approach is similar to that of Ivakin and Lysanov,[8] who employed a somewhat cruder slope averaging technique. The complete model for the high-frequency bottom backscattering cross section will be taken as the sum of the roughness and volume expressions.

Several assumptions are inherent in such an approach. First, correlations between the portions of the scattered field owing to interface roughness and sediment inhomogeneities are neglected. This is reasonable, since the volume scatterers are distributed over distances considerably greater than the acoustic wavelength, which should randomize the phase between interface and volume fields.

Equation (41) assumes that multiple scattering is negligible; i.e., the acoustic energy incident upon each elemental volume is computed by considering transmission and refraction of the incident energy at the interface, as well as attenuation in the sediment, but energy scattered by the rest of the sediment is assumed to be negligible. The single scattering assumption is valid if attenuation in the sediment is due mostly to absorption, rather than scattering of energy. Attenuation is related to the scattering and absorption cross sections in the following way (see, e.g., Ref. 21, Chap. 8):

$$\alpha_b = (10/\ln 10)(\sigma_{vt} + \sigma_a). \tag{44}$$

The quantities σ_{vt} and σ_a are *total* cross sections per unit volume for scattering and absorption by the sediment. If scattering is isotropic,

$$\sigma_{vt} = 4\pi\sigma_v. \tag{45}$$

Even if scattering is not isotropic, this expression provides a means of estimating the magnitude of the total scattering cross section. Such an estimate is needed to test the single scattering assumption, which should be valid if the *albedo* is smaller than 0.2.[54] The albedo a is defined as follows:

$$a = \sigma_{vt}/(\sigma_{vt} + \sigma_a). \tag{46}$$

Combining Eqs. (44)–(46), the following approximate condition for validity of the single scattering assumption can be obtained:

$$(\sigma_v/\alpha_b) < 0.004. \tag{47}$$

This inequality is particularly convenient, because the ratio σ_v/α_b appears in the scattering strength [Eq. (41)] and is readily determined by fitting backscatter data.

An additional approximation, closely related to the single-scattering assumption, is that the influence of the small-scale interface roughness on the acoustic field within the sediment is negligible. This is reasonable, since the small-scale surface has already been assumed (in the composite roughness model) to produce only a small perturbation to the field scattered by the large-scale surface.

Equation (41) predicts an abrupt rise in sediment volume scattering as the grazing angle increases past the critical value and penetration into the sediment becomes significant. As noted in Sec. II, interface scattering shows the opposite behavior, so there is a tendency for the sum of the two scattering processes to have a relatively small change near the critical angle. As will be seen in the next section, critical angle effects are further washed out by the slope averaging process.

VI. COMPARISON WITH DATA

Our complete model for the bottom backscattering cross section consists of two terms, one for interface scattering and one for sediment volume scattering. The interface term is to be computed by numerical integration, using Eq. (21) for grazing angles smaller than 70° and Eq. (38) for angles larger than 70°. The volume term is computed by numerical integration of Eq. (21) with $\sigma_{vs}(\theta)$ in place of $\sigma_s(\theta)$ and is applicable over the range of both moderate and steep angles. The model uses five parameters—sound speed ratio v, density ratio ρ, roughness parameters β and γ, and volume scattering parameter σ_v/α_b.

We will compare this model with the high-frequency bottom backscatter data of Jackson *et al.*[31] taken at three sites at which supporting data on roughness are available. One of these sites was in Puget Sound (US) and had a soft, silty bottom. The other two sites were in the vicinity of Falmouth (UK) and had sand bottoms. Roughness data for the Puget Sound site were measured by Igarashi and Allman,[30] who obtained a power-law exponent $\gamma = 3.5$. *In situ* measurements of sediment sound speed are also available for this site.[55] The Falmouth roughness measurements were reported by Jackson *et al.*,[31] and can be fit by the exponent $\gamma = 3$. We estimate mass density for the Puget Sound site by inserting the measured sound speed in a relation given by Hamilton and Bachman.[23] Density and sound speed were estimated for the Falmouth sites using measured sediment grain size in relationships also due to Hamilton and Bachman.

The sediment volume parameter was not measured at any of the sites, but α_b was measured at Puget Sound.[55] Whenever the measured parameters showed significant depth dependence, we chose values appropriate to depths of 10–20 cm into the sediment. This was done to favor modeling of scattering at the water–sediment interface. Volume interaction is expected to be localized near the interface as well, because the attenuation coefficient α_b falls in the neighborhood 5–20 dB m^{-1} for these sites and refraction is away from the normal ($\nu > 1$).

Figures 7 and 8 compare backscatter data from the three sites with model predictions. In these comparisons, there is only one free parameter, the ratio σ_v/α_b. The two Falmouth sites were so similar in their measured surficial properties that a single application of the model is used for both. Site 1 could be distinguished from site 2, however, in having a very thin sand layer (about 10 cm) over red sandstone. This sandstone was soft enough to be penetrated to a depth of approximately 2 cm by a gravity corer.

To separate the relative contributions of roughness and volume scattering, we give curves for the sum of both processes and for roughness scattering alone. For roughness scattering, the separate pieces of the curve computed using the composite roughness and Kirchhoff approximations splice together reasonably well at 70°. The conditions for validity of the composite roughness model are well satisfied for the soft sediment site (Fig. 7) over the grazing angle range 30°–50°. In particular, it is possible to find a cutoff wavenumber such that the Rayleigh–Rice and Kirchhoff criteria are comfortably satisfied, and the roughness statistics are Gaussian to a good approximation.[34] It is difficult to escape the conclusion that the 10 dB difference between the measured scattering strength and that predicted by the composite roughness model can only be accounted for by sediment volume scattering. The volume scattering model gives a reasonable fit for the choice $\sigma_v/\alpha_b = 0.002$, which is below the limit set by the single scattering criterion [Eq. (47)]. The backscatter data for the Puget Sound site show little frequency dependence over the frequency range 20–80 kHz, which implies the ratio σ_v/α_b is independent of frequency. Using the measured attenuation coefficient,[55] this implies a volume scattering cross section σ_v that increases in proportion to $f^{0.7}$. An increase in proportion to f^4 would indicate Rayleigh scattering from inhomogeneities much smaller than the acoustic wavelength while frequency independence would indicate geometric scattering from inhomogeneities much larger than the acoustic wavelength. Apparently the inhomogeneities responsible for scattering have a range of sizes both smaller and larger than the acoustic wavelength.

Backscatter data from other soft sediment sites[56–58,31] are often similar in level and frequency dependence to the Puget Sound data. If it can be assumed that the roughness of these sites is not unusually large, it follows that $\sigma_v/\alpha_b \approx 0.002$ for most soft sediment sites. It should be noted that a few soft sediment sites show very low backscattering strength,[56,57] indicating that σ_v/α_b is sometimes as small as 10^{-4}. The Puget Sound site had a high level of biological activity, which may account for the strong sediment volume scattering observed. It is possible that sites with low levels of biological activity will have more homogeneous sediments and little volume scattering.

The roughness scattering model accounts for most of the scattering at the two Falmouth sites. Differences between the model and the data fall slightly outside the un-

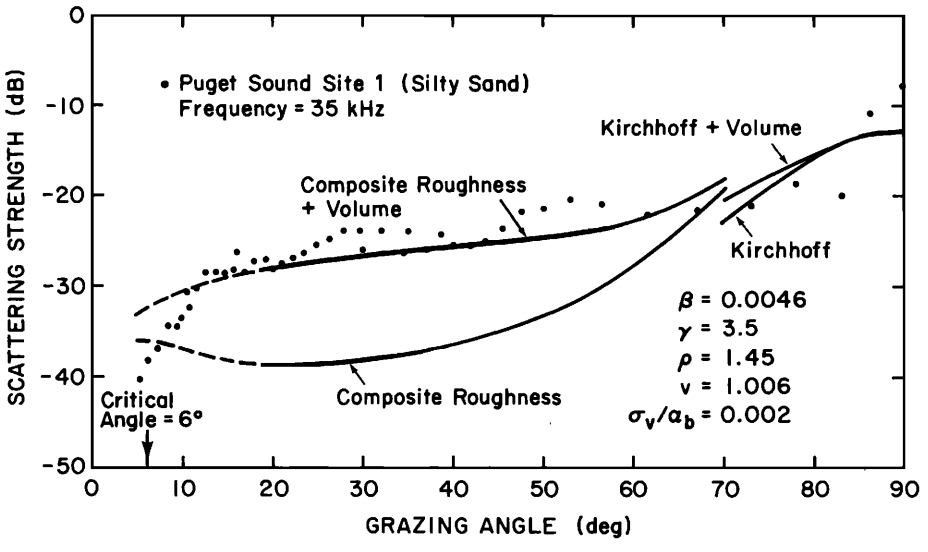

FIG. 7. Comparison of model and data for Puget Sound site 1.

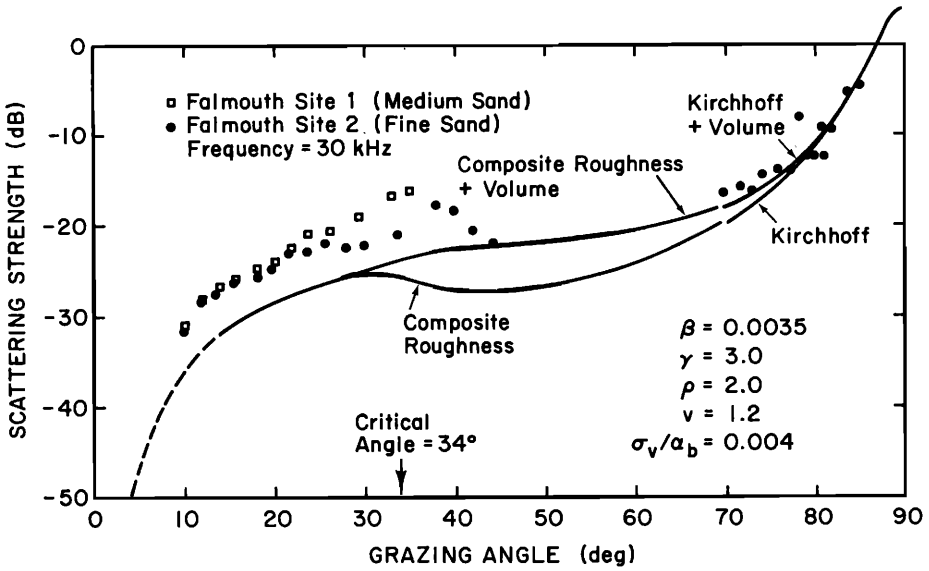

FIG. 8. Comparison of model and data for Falmouth sites 1 and 2.

certainty in the acoustic data (estimated at 3 dB), but the agreement is reasonably good. Regarding the validity of the assumptions used in our roughness scattering model, the Rayleigh–Rice and Kirchhoff criteria are satisfied, but no tests have been made for isotropy of interface roughness. There is a possibility that sand ripples were present at Falmouth site 1. The high-resolution relief data for the two Falmouth sites have not been tested for Gaussian statistics. If sharply crested sand ripples were present, the roughness statistics would not be Gaussian, because Gaussian random processes do not have the phase correlations between different frequency components required to form sharp crests. Such non-Gaussian behavior presents no difficulty for the present model if the non-Gaussian behavior is limited to the small-scale portion of the relief. As noted earlier, the small-roughness perturbation approximation used here is valid for non-Gaussian statistics provided the Rayleigh–Rice roughness criterion is met. If the large-scale portion of the relief also exhibits non-Gaussian behavior, the present model is not applicable, because the roughness power spectrum does not provide a sufficient description of the roughness statistics.[59,60]

Experimental uncertainty prevents an accurate determination of the sediment scattering parameter for the Falmouth sites. A value $\sigma_v/\alpha_b = 0.004$ was used in Fig. 8, but the true value could fall anywhere in the range below 0.01. The Falmouth sites show backscattering similar to many of the sandy sites reported in the literature.[56–58,61,62] Considering frequency dependence, Boehme *et al.*[61,62] find that many sandy sites have backscattering strength increasing roughly as 3–4.5 dB per octave, while the increase for Falmouth is 2 dB per octave with an experimental uncertainty of $\pm$ 2 dB.[31] Considering grazing angles below the critical value, our model predicts an increase of approximately 3 dB per octave.

Model and data agree in showing no dramatic effects near the critical angle. In the model, this comes about if the fitting process demands that the volume scattering term be similar in magnitude to the roughness term. If the volume scattering term is relatively small, the result is a scattering strength curve with a maximum in the vicinity of the critical angle. There are indications of this type of behavior in the tank experiment of Nolle *et al.*[2] at very high frequencies and in the deep ocean data of Patterson[1] at 2.5 kHz and Smailes[63] at 2 kHz.

The extended model agrees with the data of Boehme *et al.*[61,62] in showing a rapid falloff as the grazing angle approaches small values. The Puget Sound data show a more rapid falloff than the extended model. As noted earlier, the extended model is based on a cutoff criterion which may or may not be valid at small grazing angles. Some of the older data in the literature do not exhibit a strong falloff at small grazing angles and further experiments are needed to resolve the differences beween the older and newer data.

VII. CONCLUSIONS AND RECOMMENDATIONS

The model developed here appears to provide a useful idealization of high-frequency bottom backscattering. We have compared the model with data from sites for which all but one of the model parameters were determined by independent measurements. The results of this comparison support the validity of the model and provide insight into the physical mechanisms responsible for bottom backscattering. In soft sediments, sediment volume scattering is likely to be more important than roughness scattering, except near normal incidence and for grazing angles smaller than the critical angle. For sand bottoms, roughness scattering is relatively more important than sediment volume scattering. For most bottoms, roughness scattering dominates near normal incidence.

More theoretical work is needed to clearly delineate the regime of validity of the composite-roughness model as applied to the two-fluid rough boundary. Small discrepancies observed between model and data may indicate the onset of difficulties in the composite roughness model at small grazing angles. Uncertainties in the data do not allow definite conclusions in this regard, however. Further tests of this model will be undertaken as soon as acoustic data from sites with sufficient physical characterization become available.

Considering remote sensing applications, it is desirable to measure backscatter strength over a wide range of angles in order to separate surface and volume effects. In principle, the two roughness spectrum parameters (power-law exponent and strength parameter) can be determined from measurements near normal incidence, preferably at two or more frequencies. It is not possible, however, to extract correlation lengths of rms relief from measured backscatter strength within the roughness regime covered by this model.

ACKNOWLEDGMENTS

This work was supported by the Office of Naval Research under contract NOO14-81-K-0095. The authors wish to thank Dr. Eric Thorsos of the Applied Physics Laboratory, University of Washington, for his helpful comments.

[1]R. E. Patterson, "Backscatter of sound from a rough boundary," J. Acoust. Soc. Am. **35**, 2010–2013 (1963).
[2]A. W. Nolle, W. A. Hoyer, J. F. Mifsud, W. R. Runyan, and M. B. Ward, "Acoustical properties of water-filled sands," J. Acoust. Soc. Am. **35**, 1394–1408 (1963).
[3]Anonymous, "Scattering from the volume of an inhomogeneous half-space," Naval Research Establishment (Canada) Report No. 63/9 (1963).
[4]E. Y. Kuo, "Wave scattering and transmission at irregular surfaces," J. Acoust. Soc. Am. **36**, 2135–2142 (1964).
[5]Yu. Yu. Zhitkovskii, "The scattering of sound by inhomogeneities of the top layer of the ocean bottom," Izvest. Atmos. Ocean. Phys. **4**, 323–325 (1968).
[6]W. A. Kuperman, "Coherent component of specular reflection and transmission at a randomly rough two-fluid interface," J. Acoust. Soc. Am. **58**, 365–370 (1975).
[7]C. S. Clay and H. Medwin, *Acoustical Oceanography: Principles and Applications* (Wiley-Interscience, New York, 1977).
[8]A. N. Ivakin and Yu. P. Lysanov, "Underwater sound scattering by volume inhomogeneities of a bottom medium bounded by a rough surface," Sov. Phys. Acoust. **27**, 212–215 (1981).
[9]P. A. Crowther, "Some statistics of the sea-bed and scattering therefrom," in *Acoustics and the Sea-bed*, edited by N. G. Pace (Bath University, Bath, 1983), pp. 147–155.
[10]C. S. Clay and W. K. Leong, "Acoustic estimates of topography and roughness spectrum of the sea floor southwest of the Iberian Peninsula," in *Physics of Sound in Marine Sediments*, edited by L. Hampton (Plenum, New York, 1974), pp. 373–446.
[11]A. D. Dunsiger, N. A. Cochrane, and W. J. Vetter, "Seabed characterization from broad-band acoustic echosounding with scattering models," IEEE J. Ocean Eng. **OE-6**, 94–106 (1981).
[12]T. K. Stanton, "Sonar estimates of seafloor microroughness," J. Acoust. Soc. Am. **75**, 809–818 (1984).
[13]J. W. Strutt (Lord Rayleigh), *The Theory of Sound* (Dover, New York, 1945).
[14]S. O. Rice, "Reflection of electromagnetic waves from slightly rough surfaces," in *The Theory of Electromagnetic Waves, A Symposium* (Interscience, New York, 1951), pp. 351–378.
[15]H. W. Marsh, "Exact solution of wave scattering by irregular surfaces," J. Acoust. Soc. Am. **33**, 330–333 (1961).
[16]H. W. Marsh, M. Schulkin, and S. G. Kneale, "Scattering of underwater sound by the sea surface," J. Acoust. Soc. Am. **33**, 334–340 (1961).
[17]H. W. Marsh, "Sound reflection and scattering from the sea surface," J. Acoust. Soc. Am. **35**, 240–244 (1963).
[18]J. W. Miles, "On nonspecular reflection at a rough surface," J. Acoust. Soc. Am. **26**, 191–199 (1954).
[19]S. T. McDaniel and A. D. Gorman, "Acoustic and radar sea surface backscatter," J. Geophys. Res. **87**, 4127–4136 (1982).
[20]S. T. McDaniel and A. D. Gorman, "An examination of the composite-roughness scattering model," J. Acoust. Soc. Am. **73**, 1476–1486 (1983).
[21]R. J. Urick, *Principles of Underwater Sound* (McGraw-Hill, New York, 1975).
[22]E. L. Hamilton, "Compressional wave attenuation in marine sediments," Geophysics **37**, 620–646 (1972).
[23]E. L. Hamilton and R. T. Bachman, "Sound velocity and related properties of marine sediments," J. Acoust. Soc. Am. **72**, 1891–1904 (1982).
[24]M. D. Richardson and D. K. Young, "Geoacoustic models and bioturbation," Marine Geol. **38**, 205–218 (1980).
[25]M. D. Richardson, D. K. Young, and R. I. Ray, "Effects of hydrodynamic and biological processes on sediment geoacoustic properties in Long Island Sound, U.S.A.," Marine Geol. **52**, 201–226 (1983).
[26]T. E. Bell, "Statistical features of sea-floor topography," Deep-Sea Res. **22**, 883–892 (1975).
[27]J. M. Berkson and J. E. Matthews, "Statistical characterization of seafloor roughness," IEEE J. Ocean Eng. **OE-9**, 48–51 (1984).
[28]C. G. Fox and D. E. Hayes, "Quantitative methods for analyzing the roughness of the seafloor," Rev. Geophys. **23**, 1–48 (1985).
[29]T. Akal and J. Hovem, "Two-dimensional space series analysis for seafloor roughness," Marine Geotechnol. **3**, 171–182 (1978).
[30]Y. Igarashi and R. L. Allman, "An acoustic bottom microprofiler and its application to high-frequency bottom scattering," J. Acoust. Soc. Am. Suppl. 1 **72**, S36 (1982).
[31]D. R. Jackson, A. M. Baird, J. J. Crisp, and P. A. G. Thomson, "High-frequency bottom backscattering measurements in shallow water," J. Acoust. Soc. Am. (submitted).
[32]A. M. Yaglom, *An Introduction to the Theory of Stationary Random Functions* (Prentice-Hall, Englewood Cliffs, NJ, 1962).
[33]A. Ishimaru, *Wave Propagation and Scattering in Random Media, Volume 2, Multiple Scattering, Turbulence, Rough Surfaces, and Remote Sensing* (Academic, New York, 1978).
[34]D. B. Percival (private communication) has tested data obtained from Igarashi and Allman (Ref. 30) for Gaussian statistics.
[35]F. M. Labianca and E. Y. Harper, "Connection between various small-waveheight solutions of the problem of scattering from the ocean surface," J. Acoust. Soc. Am. **62**, 1144–1157 (1977).
[36]J. G. Watson and J. B. Keller, "Reflection, scattering, and absorption of acoustic waves by rough surfaces," J. Acoust. Soc. Am. **74**, 1887–1894 (1983).
[37]D. E. Barrick and W. H. Peake, "Scattering from surfaces with different roughness scales: Analysis and interpretation," Battelle Memorial Institute Report BAT-197A-10-3 (1967).
[38]G. S. Brown, "Backscattering from a Gaussian-distributed, perfectly conducting rough surface," IEEE Trans. Antennas Propagat. **26**, 472–482 (1978).
[39]G. S. Brown, "Correction to backscattering from a Gaussian-distributed perfectly conducting rough surface," IEEE Trans. Antennas Propagat. **28**, 943–946 (1980).
[40]R. J. Wagner, "Shadowing of randomly rough surfaces," J. Acoust. Soc. Am. **41**, 138–147 (1967).
[41]W. Bachmann, "A theoretical model for the backscattering strength of a composite-roughness sea surface," J. Acoust. Soc. Am. **54**, 712–716 (1973).
[42]F. G. Bass and I. M. Fuks, *Wave Scattering from Statistically Rough Surfaces* (Pergamon, Oxford, 1979), p. 438.
[43]M. L. Burrows, "A reformulated boundary perturbation theory in electromagnetism and its application to a sphere," Can. J. Phys. **45**, 1729–1743 (1967).
[44]D. P. Winebrenner, "A surface field phase perturbation method for scattering from rough surfaces," Ph.D. dissertation, University of Washington, 1985.
[45]N. N. Galybin, "Back scattering of sound by a disturbed sea surface," Sov. Phys. Acoust. **22**, 193–197 (1976).
[46]E. G. Liszka and J. J. McCoy, "Scattering at a rough boundary—Extensions of the Kirchhoff approximation," J. Acoust. Soc. Am. **71**, 1093–1100 (1982).
[47]S. T. McDaniel, "Diffractive corrections to the high-frequency Kirchhoff approximation," J. Acoust. Soc. Am. **79**, 952–957 (1986).
[48]M. V. Berry and T. M. Blackwell, "Diffractal echoes," J. Phys. A: Math. Gen. **14**, 3101–3110 (1981).
[49]C. S. Clay, "Fluctuations of sound reflected from the sea surface," J. Acoust. Soc. Am. **32**, 1547–1551 (1960).
[50]C. W. Horton, Sr. and D. R. Melton, "Importance of the Fresnel correction in scattering from a rough surface. Part II. Scattering coefficient," J. Acoust. Soc. Am. **47**, 299–303 (1970).
[51]Yu. P. Lysanov, "Criterion defining the 'far zone' in wave scattering by statistically rough surfaces," Sov. Phys. Acoust. **17**, 74–76 (1971).
[52]N. G. Pace, Z. K. S. Al-Hamdani, and P. D. Thorne, "The range depen-

dence of normal incidence acoustic backscatter from a rough surface," J. Acoust. Soc. Am. **77**, 101–112 (1985).
[53]D. P. Winebrenner and A. Ishimaru, "On the far field approximation for scattering from randomly rough surfaces," IEEE Trans. Antennas Propagat. (accepted for publication).
[54]F. T. Ulaby, R. K. Moore, and A. K. Fung, *Microwave Remote Sensing, Active and Passive, Vol. II* (Addison–Wesley, Reading, MA, 1982), p. 888.
[55]Y. Igarashi and R. L. Allman, "Sound speed and attenuation in marine sediments measured at high frequencies with a bottom probe system," J. Acoust. Soc. Am. Suppl. 1 **72**, S98 (1982).
[56]C. M. McKinney and C. D. Anderson, "Measurements of backscattering of sound from the ocean bottom," J. Acoust. Soc. Am. **36**, 158–163 (1964).
[57]H.-K. Wong and W. D. Chesterman, "Bottom backscattering near grazing incidence in shallow water," J. Acoust. Soc. Am. **44**, 1713–1718 (1968).
[58]A. V. Bunchuk and Yu. Yu. Zhitkovskii, "Sound scattering by the ocean bottom in shallow-water regions (review)," Sov. Phys. Acoust. **26**, 363–370 (1980).
[59]C. S. Clay, H. Medwin, and W. M. Wright, "Specularly scattered sound and the probability density function of a rough surface," J. Acoust. Soc. Am. **53**, 1677–1682 (1973).
[60]W. A. Kinney and C. S. Clay, "Insufficiency of surface spatial power spectrum for estimating scattering strength and coherence: Numerical studies," J. Acoust. Soc. Am. **78**, 1777–1784 (1985).
[61]H. Boehme, N. P. Chotiros, L. D. Rolleigh, S. P. Pitt, A. L. Garcia, T. G. Goldsberry, and R. A. Lamb, "Acoustic backscattering at low grazing angles from the ocean bottom. I. Bottom backscattering strength," J. Acoust. Soc. Am. **77**, 962–974 (1985).
[62]H. Boehme, N. P. Chotiros, and N. D. Churay, "Bottom acoustic backscattering at low grazing angles in shallow water. Part I. Bottom backscattering strength," in *Scattering Phenomena in Underwater Acoustics*, Proc. Inst. Acoust. **7** (Pt. 3), 19–26 (1985).
[63]I. C. Smailes, "Bottom reverberation measurements at low grazing angles in the NE Atlantic and Mediterranean Sea," J. Acoust. Soc. Am. **64**, 1482–1486 (1978).